Published in final edited form as:
J Air Waste Manag Assoc. 2019 June ; 69(6): 752–763. doi:10.1080/10962247.2019.1580229.

Power Models and Average Ship Parameter Effects on Marine Emissions Inventories

Isabela N. Brown and
ORISE research participant at the U.S. Environmental Protection Agency, Ann Arbor, MI, USA

Michael F. Aldridge
U.S. Environmental Protection Agency, Ann Arbor, MI, USA

Introduction

Between 2007 and 2012, shipping accounted for an average of 2.8 percent of global greenhouse gas emissions. By 2050, these maritime emissions are projected to increase by 50 percent to 250 percent (International Maritime Organization, 2014). To better analyze these trends, an understanding of common marine emission model methods, and their impacts, is required. All activity-based marine emission models include an estimation of ship propulsive power, for which multiple methods, of varying degrees of complexity, are available. Most of the marine emissions inventories of the last ten years have estimated power using variations on the Propeller Law (EPA,2009a) (EPA,2009b) (Starcrest,2016) (Starcrest,2017) (MacKay,2015) (Yau,2012) (Goldsworthy,2015).

A Propeller Law methodology was originally pursued in part for its simplicity, at a time when comprehensive vessel activity data was unavailable. However, recent years have seen an emergence of Automated Identification System (AIS) ship activity data in marine emissions modeling methodology. AIS supplies detailed vessel speed, draft and location information, along with vessel identifications. This influx of data has allowed the Propeller Law to be analyzed according to reported, rather than assumed, speeds. In addition, over the last five years, several inventories have been calculated using power models that are more complex than the Propeller Law (International Maritime Organization, 2014) (Scarbrough et al., 2017) (Winther et al., 2014) (Jalkanen et al., 2012).

Simple, load-factor-based power models have often been regarded in marine emissions inventories as roughly representative of more complex methods (Goldsworthy, 2015) (International Maritime Organization, 2014). Complex models are often avoided due to their large number of required inputs and are likely more feasible with the use of averaged ship parameters for gap filling (Nunes et al., 2017). However, the impact of applying these different power models on marine emissions inventories has yet to be fully evaluated. This paper examines the effects of two complex, resistance-based and two simple, load-factor-based, propulsive power models on calculating baseline emissions inventories with unique vessel parameters. CO_2 emissions were calculated for each inventory using the Propeller Law, Admiralty Law, Holtrop & Mennen method, and Kristensen method (EPA,2009a) (EPA,2009b) (International Maritime Organization, 2014) (Holtrop & Mennen, 1982) (Kristensen 2016). In addition, to determine the effect of applying averaged ship parameters

on emissions inventories, an average hull inventory was compiled by replacing all individual ship characteristics in the baseline inventory with values averaged by ship subtypes.

Power Models

Propeller Law

Most available marine emissions inventories have modeled power demand based on the Propeller Law (Eq.1) where P is the engine power required to drive a propeller with speed of V, and the coefficients c and n define the proportionality between the two.

$$\mathrm{P} = c \times V^n \quad (1)$$

The accuracy of this model may change with hull fouling, engine efficiency, and weather effects; however, it has been shown to produce reasonable estimations of engine power (Molland, 2011) (MAN Diesel & Turbo, 2011). Replacing engine power and propeller speed with ship required power and vessel speed reduces the accuracy of this relationship (MAN Diesel & Turbo, 2011). Most marine emissions inventories based on the Propeller Law have used an adapted version, where a relative engine load factor (LF) is calculated from the cubed ratio of the ship's speed (V) to a reference speed (V_{ref}) (Eq. 2) (EPA,2009a) (EPA, 2009b) (Starcrest,2016) (Starcrest,2017) (MacKay,2015) (Yau,2012) (Goldsworthy,2015).

$$P = \mathrm{LF} \times P_{ref} = \left(\frac{V}{V_{ref}}\right)^3 \times P_{ref}$$

The load factor is assumed to be equal to the ratio of the ship's required power at speed V, and the power required (P_{ref}) for the ship to travel at the reference speed. P_{ref}, at service speed, is modeled as 83 percent of total installed propulsive power (EPA, 2009a).

This approach assumes that that the cubic relationship (n=3) and the proportionality (c) between vessel speed and power demand would remain constant for all speeds and ship types. However, studies have shown that both n and c are affected by ship type and speed (Schneekluth, 1998) (MAN Diesel & Turbo, 2011). Using a load factor based on the Propeller Law has the benefit of requiring few inputs while reflecting general speed-power relationships used by engine manufacturers. Additionally, the load factor formula anchors the calculated power around well documented relationships between engine power and speed at the ship's service speed. However, the Propeller Law does not capture significant influences on ship power such as hull shape, cargo load, and engine efficiency.

Admiralty Law

One alternative to the Propeller Law is the Admiralty Law, where *Disp* is the ship hull displacement and A is the admiralty coefficient (Eq. 3).

$$\mathrm{P} = \frac{Disp^{\frac{2}{3}} \times V^{n}}{A} \quad (3)$$

The admiralty coefficient is considered a rough approximation of the relationships between ship hull parameters, speed and power (Harvald, 1983) (Schneekluth,1998) (Molland, 2011) (MAN Diesel & Turbo, 2011). Some recent emissions inventories have begun to implement an Admiralty Law load factor (Eq.4), by substituting draft (T) for displacement (International Maritime Organization, 2014) (Scarbrough et al., 2017).

$$\mathrm{P} = \mathrm{LF} \times P_{ref} = \left(\frac{T_{reported}^{\frac{2}{3}} \times V_{reported}^{3}}{T_{ref}^{\frac{2}{3}} \times V_{ref}^{3}} \right) \times P_{ref} \quad (4)$$

The Admiralty Law load factor is mathematically equivalent to the Propeller Law load factor when vessels are modeled as operating at their maximum draft. As such, the Propeller Law load factor acts as an upper bound to the Admiralty Law load factor. Some advantages of the Admiralty Law load factor include its minimal required inputs, and its ability to account for an approximation of hull wetted surface area, via the draft parameter. Like the Propeller law, the Admiralty Law anchors engine power estimates to the relationship between service speed and service power. However, it does not account for the effect of speed and hull shape on the changing exponential relationship (n) between ship speed and power (Schneekluth, 1998). Additionally, the effects of engine efficiency, and of hull shape on hull wetted surface area, are not accounted for (Schneekluth,1998).

Resistance-Based Models

Resistance-based models of ship power typically follow the form of equation 5, where C_T is the total ship hull resistance coefficient, ρ is sea water density, S is the hull wetted surface area, and η_T represents engine efficiency.

$$\mathrm{P} = \frac{\rho \times C_T \times \frac{1}{2} \times S \times V_{reported}{}^{3}}{\eta_T} \quad (5)$$

This study analyzes two resistance-based models, one developed by Holtrop & Mennen and the other by Kristensen (Holtrop & Mennen, 1982) (Kristensen, 2016). Holtrop & Mennen developed one of the first numerical resistance-based models in 1982 through regression analysis of tank towing data from the Netherlands Ship Model Basin (Holtrop & Mennen, 1982). Their model is well referenced in naval architecture literature and has been implemented and analyzed in recent inventory work (Rakke, 2016) (International Maritime

Organization, 2014). A more recently developed resistance-based model is Kristensen's SHIP-DESMO model (Kristensen 2016), which is an evolution of Harvald's 1982 tank towing regression analysis, and has been used in recent inventories (Harvald, 1982) (Winther et al., 2014). Other inventories, such as Jalkanen et al. (2012) (2014), have also included resistance-based power models in their methods and have been recommended for use (Nunes et al., 2017). However, these require inputs which were not easily accessible through ship parameter and activity datasets.

The Holtrop & Mennen total hull resistance is calculated as described in equation 6, in which the resistance components R_W, R_B, R_{Tr}, C_F, FormFactor, and C_A are described as functions of their input vessel parameters.

$$
\begin{aligned}
&C_{T_{HoltropMennen}} = \\
&R_w\left(V_{reported}, Breadth, \quad C_B, \quad T_{Ref}, T_{Reported}, \quad Disp_{Max}, lwl, Ship \quad Type, \quad \rho\right) \\
&+ \quad R_B\left(V_{reported}, Breadth, C_B, T_{Ref}, T_{Reported}, Ship \quad Type, \rho\right) \\
&+ \quad R_{Tr}\left(V_{reported}, Breadth, C_B, T_{Ref}, T_{Reported}, Ship \quad Type, \rho\right) \\
&+\left(\frac{1}{2} \times \rho \times S \times V_{reported}{}^2\right) \\
&\times \Big[\quad C_F\left(V_{reported}, Lwl, Temp, \rho\right) \\
&\times \quad FormFactor\left(T_{Ref}, T_{Reported}, Lwl, \quad Breadth, Disp_{Max}, \quad Ship \quad Type, C_B\right) \\
&+ \quad C_A\left(T_{Ref}, T_{Reported}, Lwl, Breadth, Ship \quad Type, C_B\right)\Big]
\end{aligned}
\tag{6}
$$

The Kristensen total hull resistance is calculated as described in equation 7, in which the resistance components C_F, C_R, C_A, and C_{AA} are described as functions of their input vessel parameters.

$$
\begin{aligned}
&C_{T_{Kristensen}} = \\
&\left[C_F\left(V_{reported}, Lwl, Temp, \rho\right)\right. \\
&+C_R\left(Ship \quad Type, C_B, \quad T_{Ref}, T_{Reported}, Breadth, \quad Disp_{Max}, \quad Lwl\right) \\
&+C_A\left(Ship \quad Type, C_B, T_{Ref}, \quad T_{Reported}, \quad Disp_{Max}\right) \\
&\left.+C_{AA}(Ship \quad Type, DWT)\right] \\
&\times\left(\frac{1}{2} \times \rho \times S \times V_{reported}{}^2\right)
\end{aligned}
\tag{7}
$$

Where,

$$Breadth = Ship \quad Breadth \quad (m)$$

$$C_A = Hull \quad Roughness \quad Resistance \quad Coefficient$$

$$C_{AA} = Air \quad Resistance \quad Coefficient$$

$$C_F = Frictional \quad Resistance \quad Coefficient$$

$$C_R = Residual/Wavemaking \quad Resistance \quad Coefficient$$

$$C_B = Block \quad Coefficient = \frac{Disp_{Max}}{lwl \times Breadth \times T_{Ref}}$$

$$Disp_{Max} = Maximum \quad Hull \quad Displacement \quad \left(m^3\right)$$

$$DWT = Deadweight \quad Tonnage$$

$$Lwl = Waterline \quad Length \quad (m)$$

$$R_B = Bulbous \quad Bow \quad Resistance \quad (kN)$$

$$R_{TR} = Immersed \quad Transom \quad Resistance \quad (kN)$$

$$R_w = Wavemaking \quad Resistance \quad (kN)$$

$$Temp = Sea \quad Surface \quad Temperature \quad (15\,℃)$$

$$T_{Ref} = Summer \quad Load \quad Line \quad Draft \quad (m)$$

$$T_{Reported} = \quad AIS \quad Reported \quad Draft \quad (m)$$

The power required to propel a vessel against frictional resistance generally increases with a cubic relationship to speed. However, resistance-based models also capture wave-making resistance, for which the relationship to ship speed is not cubic and varies significantly (MAN Diesel & Turbo, 2011). Additionally, these methods account for the effect of hull shape on hull wetted surface area and hull resistance. Because of this, the resulting relationship between the estimated power demand and vessel speed changes according to ship speed and ship type for both resistance-based methods. Unlike the load-factor-based models, resistance-based models are not inherently anchored to the engine's service power. Ideally, resistance-based models should be calibrated against in-use data from full-sized vessels. Resistance-based power models require a larger number of inputs (listed in Tables 1–3) and calculation steps than the load-factor-based approaches. However, these models allow for greater flexibility in modeling the impact of ship hull design, and speed ranges, on propulsive engine load and thus emissions.

The International Maritime Organization (IMO) Greenhouse Gas Study conducted a comparison of the Holtrop & Mennen and Admiralty Law load factor models (IMO, 2014). The study calculated the values of the exponent (n) in the Admiralty Law load factor equation for a sample of ships and speeds such that the model agreed with power estimates from the Holtrop & Mennen model. This analysis showed that exponential relationships where $n \geq 3$ create the best agreement between the two models. Because the exponent, n, is applied to a load factor with a value less than or equal to one, a larger exponent indicates a decrease in modeled power. The IMO study determined that a cubic relationship ($n = 3$) is preferable for larger bulk carriers, while higher values are preferable for smaller container ships. These findings are consistent with recommendations supplied by MAN Diesel & Turbo (2011) regarding how the speed-power relationship within the Propeller Law could best represent hull resistance. MAN Diesel & Turbo recommended an exponent of 3.2 for slow-speed bulk carriers and tankers, 3.5 for medium-speed feeder container ships, reefers, and ro-ros, and 4 for high-speed container ships.

Beyond these studies, little analysis been done on the relative differences between these models, and on the effect of model selection on the magnitude of calculated emissions. The following analysis compares the emissions estimates generated using these four power models. Additionally, the impact of using average ship characteristics, rather than ship-specific ones, as model inputs, is assessed.

Methodology

Sample Fleet

Six months of AIS data for vessels operating off the coast of the southwestern United States was acquired from the United States Coast Guard (USCG) for analysis. The sample area is bounded by the rectangle defined by 38.242 ^{O}N −116.796 ^{O}W, and 32.6703 ^{O}N −128.296 ^{O}W. This sample region contains the ports of Los Angeles and Long Beach to the south and the port of Oakland to the north. To the west, this area extends just beyond the boundary of the North American Emission Control Area. This region was selected for its high level of ship traffic which would yield a suitably large sample of vessels for this study. Additionally, the selected region captures a wide range of ship activity from port operations, to near coast traffic within the California Vessel Speed Reduction Zone (VSR), as well as higher speed cruise activity further from the coast. Container ships, tankers, and bulk carriers were sampled, as these ship types represent those most commonly used in national commerce (United States Army Corps of Engineers, 2017). Only vessels for which all necessary ship parameter data (see Tables 1–3) was available were considered in this analysis, to avoid the effect of vessel parameter assumptions. Vessels reporting outlier speeds, greater than 30 knots, or with missing reported speeds, were excluded from the analysis. In total, the sample was comprised of records from 248 unique vessels.

The AIS dataset used for this study is aggregated to five-minute intervals but sometimes includes gaps between messages greater than five minutes. For this analysis, vessels were assumed to operate at the same speed as the message prior to the gap for the duration of the missing period. If the position and heading of the ship associated with a gap between messages indicated that the ship had traveled outside of the sample area, no activity was assumed during that gap. Data from IHS Fairplay was used to capture the full range of ship parameters needed for the four models, as this methodology is consistent with common inventory practices (IHS Maritime Fairplay, 2014) (International Maritime Organization, 2014) (Starcrest, 2017). Likewise, ship types were determined by the Lloyds Stat 5 code from the same data set. The parameters were initially matched to the AIS data by IMO Number. If IMO numbers were not available, Maritime Mobile Service Identity (MMSI) numbers were used.

At-berth and anchorage operations were defined as all vessel activity at or below three knots and categorized as hotelling (International Maritime Organization, 2014). Hotelling activity accounts for the majority of records in the AIS sample, reflecting 72 percent, 56 percent, and 75 percent of bulk carrier, container ship and tanker time, respectively. The propulsive power required for these operations is minimal, and often is calculated as zero required power, at zero knots, or is bounded at 2 percent of total power. Given that hoteling propulsive power is bounded regardless of power model, the effect of power model selection on hoteling emissions is minimal, and these emissions have been omitted from the scope of this study.

The speed distribution (>3kn) of the sample fleet, using one knot speed bins, is plotted in Figure 1, along with the distribution of the ratio of reported AIS speed to vessel service speed for each message. Here service speed is defined as 94 percent of maximum vessel speed and is generally considered the speed at which load-factor-based models are most

accurate (EPA, 2009a) (Goldsworthy, 2015). Most container ships continue to operate well below their service speed while bulk carriers and tankers consistently operate at 90 percent of their service speed. The speed distributions of all three ship types peak around 12 knots, the maximum speed allowed for vessels to receive benefits from the Port of Los Angeles and Long Beach's Vessel Speed Reduction Program (Starcrest, 2017).

Reported draft is a necessary input into the Admiralty, Holtrop & Mennen, and Kristensen power models. This analysis uses the AIS reported draft for vessel trips, following the methodology of the Third IMO Greenhouse Gas Study (2014). Figure 2 demonstrates the ratio between the reported and summer load line drafts of the sample fleet. The transits analyzed in Figure 2 are defined by observed trips from AIS activity. The bimodal distributions of draft reported by tankers and bulk carriers indicate that these ships typically operate at nearly full capacity or near ballast conditions.

Tables 1–3 summarize the time-weighted average and relative standard deviations of the sample fleet's ship parameters by ship type and subtype groupings. Subtypes represent ship type size classes categorized by the given deadweight tonnage (dwt) ranges, as defined by Kristensen, along with the TEU to dwt ratios for container ships (Kristensen, 2017a, 2017b, 2017c). Few large tankers exist within the sample, resulting in small relative standard deviations for their parameters. Larger variances surround hull displacement, deadweight tonnage, and total propulsive power for this sample fleet. Tankers display the highest variance in reported draft, as is also seen in Figure 2.

Inventory Calculations

A baseline ship fleet was created by compiling the above-mentioned vessels, their unique ship parameters, and their message by message AIS activity profiles. In addition, an average hull fleet was created using the average hull parameters from Tables 1–3. For this fleet, each vessel in the baseline fleet was assigned the average hull parameters of their respective ship type and subtype groups. The accuracy of the average hull fleet increased significantly when average block coefficients (C_B), which describe the "blockiness" of the hull, were applied to the fleet instead of being calculated by average displacement, breath, length and draft parameters.

Four inventories were developed for the baseline and average hull fleets by calculating power demand according to Propeller Law, Admiralty Law, Holtrop & Mennen, and the Kristensen models. Propulsive power was calculated for each time interval between consecutive AIS messages of all vessels in the sample fleet. For each five-minute interval, vessels were assumed to operate at the same speed and draft as the message at the beginning of the period. The Propeller and Admiralty Laws were modeled using the load factor equations presented above. The Holtrop & Mennen model was calculated with the assumptions described in Rakke (2016). The Kristensen model was calculated according to the assumptions used in the associated SHIP-DESMO excel model (Kristensen, 2017d). An R package was developed to apply each of these models to the sample fleet and to aggregate the results. As this analysis was intended to assess impact of propulsive power models on calculated emissions, it ignored additional vessel energy usage, such as auxiliary engine, and shaft generator loads. For simplicity, no service margin was included and sea surface

temperature of 15°C was assumed. Likewise, although some resistance-based models include acceleration and shallow water effects, these have been omitted from the current analysis (Jalkanen, 2012) (Lackenby, 1963) (Kristensen, 2017d).

A lower bound of 2 percent, and an upper bound of 100 percent, of total installed power, was applied to these estimates of ship power demand (EPA, 2009a). Low load adjustment factors (LLAF) account for the decrease in engine efficiency during low loads. They were applied to vessel emissions estimates for which modeled power was less than or equal to 20 percent of total installed power. The EPA (2009a) provided CO_2 LLAF is calculated from the load factor using equation 8.

$$LLAF_{CO_2} = 44.1(\quad LF)^{-1} + 648.6. \quad (8)$$

Because CO_2 emissions are directly correlated to engine power output and efficiency, they were chosen as the most appropriate metric to compare these models. All sampled vessels were determined to have slow speed diesel (SSD) engines, which are primarily identified as two stroke engines, or as engines operating at speeds less than or equal to 500 rpm if stroke type was unknown. With some exceptions, there is generally a broad rpm band separating slow and medium speed diesel engines, however the 500 rpm cutoff was deemed most appropriate to separate these two groups (Diesel & Gas Turbine, 2013). Equation 8 is derived from medium-speed engines, however it is applied to the SSD fleet at hand for consistency with standard inventory practices (Starcrest, 2017) (International Maritime Organization, 2014). The ENTEC (2002) category 3 CO_2 emission factor for SSD engines is 620.62 g/kWh, which reflects an assumption of residual fuel usage by the entire sample fleet. Emissions were calculated per AIS message interval using equation 9:

$$Emissions_{CO_2} = EF_{CO_2} \times \quad LLAF_{CO_2} \times \quad P \times \quad \Delta t \quad (9)$$

where EF_{CO2} is the base emission factor, and Δt is the time between consecutive AIS messages.

Results

Inventories

Power Model Selection Impacts—Figure 3 summarizes the total non-hotelling CO_2 emissions calculated for the baseline fleet using each power model. Due to its widespread use in published marine emissions inventories, the Propeller Law model is chosen as a reference for comparison. Table 4 describes the percent difference in emissions estimates from that of the Propeller Law inventory. The Holtrop & Mennen model deviates the furthest from the Propeller Law and the Admiralty Law deviates the least. Deviations from Propeller Law CO_2 estimates range from −9.5 percent to −42.4 percent.

Calculations using the Admiralty Law result in estimated emissions ranging from 9.5 percent to 18.1 percent lower than those calculated using the Propeller Law. As previously noted, this is because the Propeller Law can be considered an upper bound for the Admiralty Law equation, which explicitly accounts for the wetted surface area of hulls that are not fully loaded. As Figure 2 shows, a large portion of container ships in the fleet were active at 90 percent of their maximum draft. This is near where the Admiralty Law converges with the Propeller Law, thus resulting in the smallest observed difference between the two models for container ships. Alternately, bulk carriers and tankers tend to operate in either fully loaded or ballast conditions. These ship type dependent operations result in much larger deviations between the Admiralty and Propeller Law estimates for these ship types.

Emissions were lowest when calculated by resistance-based models. Like the Admiralty Law, resistance-based models account for the wetted surface area of hulls that are not fully loaded, and thus estimate lower CO_2 emissions than the Propeller Law does for this fleet. As previously noted, the Third IMO Greenhouse Gas Study has shown that Admiralty Law load factor exponents (n) need to be increased for its results to agree with those of Holtrop & Mennen. An increase in an exponent applied to a fractional engine load results in decreased Holtrop & Mennen modeled power with respect to the Admiralty Law, which Figure 3 reflects.

These differences between the power models are best demonstrated by comparing total calculated emissions as a function of ship speed. Figure 4 plots percent differences in total emissions estimates from the Propeller Law by speed bin (0.5 knots bins).

Near the service speed, hull resistance is dominated by frictional resistance, which is generally proportional to the cube of the ship’s speed (MAN Diesel & Turbo, 2011). Therefore, at the service speed, the Admiralty Law roughly approximates the influences of the hull wetted surface area and the frictional resistance that are calculated by the resistance-based models. The resistance-based models account for the effect of wave-making resistance which becomes exponentially significant relative to the overall power demand as ship speed increases beyond the service speed (MAN Diesel & Turbo, 2011). Because of this, Figure 4 shows resistance-based modeled power increasing toward, and at times surpassing, the Propeller Law power estimations at high speeds. The Admiralty Law does not take wave-making resistance into account, and thus, at higher speeds, its modeled power does not increase relative to the Propeller Law.

The effect of wave-making resistance is even more significant for high speed container ships than it is for tankers or bulk carriers (MAN Diesel & Turbo, 2011). However, the AIS activity profiles show the sample fleet container ships operating at speeds much lower than their rated service speed (Figure 1). For this reason, and because most container ships in the sample operate fully loaded, the observed deviations between modeled emissions are smallest for container ships.

Effect of Applying Average Hulls—The above analysis indicates that power model selection can significantly impact inventory emissions estimates. Thus, the integration of these models into inventory methodology should be evaluated. Resistance-based models are

typically avoided due to the number of required inputs (Nunes et al., 2017). As of yet, no study has documented their sensitivities to average ship parameters. Average ship hull inventories were computed using exclusively subtype averaged hull characteristics and were compared to the baseline estimates for each ship type and power model. The percent difference in the emissions estimates of these two inventories are plotted in Figure 5.

This analysis indicates that use of subtype averaged ship parameters would result in less than a 2.5 percent difference in emission estimates for a given AIS sample of this size. Furthermore, the analysis showed that the Propeller Law model is the most sensitive to average bulk carrier total installed propulsive power, which has a high level of variance (Table 1). Holtrop & Mennen was the least impacted by average ship parameters, while the Kristensen model saw sensitivities to average hull displacement. In comparing the effect of each average ship parameter to the effect of the entire average hull, it was determined that more accurate results were obtained when just one, rather than all, parameters were replaced by subtype averaged values.

Individual Vessels

Power Model Selection Impacts—As inventories range in scope and size, it is crucial to understand the impact of power model selection when estimating emissions for individual vessels. The results of the Propeller Law were compared to those of the remaining models for each unique vessel in the sample (Figure 6).

Predicted emissions deviations from the Propeller Law increase when considering emissions from individual vessels as compared to the inventory of the entire fleet. These differences for unique vessels range at times up to 70 percent, however on average fall within a 40 percent range. Like inventory-wide comparisons, most sampled vessels saw a decrease in estimated emissions relative to results from the Propeller Law. This is likely due to the use of AIS reported draft, and the low engine loads resulting from resistance models at low speeds.

This relationship is evident by examining outlier vessels. Outlier vessels were described as having higher emissions by resistance-based models than by the Propeller Law. The characteristics of these outlier vessel messages are plotted in Figure 7 and represent either reported speeds greater than the service speed, or vessels with fully loaded hulls. As described above, the Propeller Law is best fit to approximate the power demand required for frictional resistance on fully loaded hulls. When resistance-based methods model such hulls, with reported draft representing 90 percent to 110 percent of summer load line draft, they account for wave-making resistance and exceed Propeller Law model estimations. Likewise, power demand for vessels at high speeds is dominated by wave-making resistance. The power required for such activity can at times exceed the demand modeled by the Propeller Law.

Effect of Applying Average Hulls—Figure 8 shows that the application of average ship parameters has a greater effect on the emissions estimates of individual vessels than of fleets. Most vessels see between a −10 percent to 20 percent difference in emissions estimates when average hull, as compared to unique, parameters are used. Whereas fleet-wide inventories are minimally impacted by averaged parameters, and significantly impacted

by power model selection, the effects of these two influences may be equivalent for some individual vessel emissions estimates. Outlier vessels can see a 50 percent to 200 percent difference in modeled emissions when average ship parameters are used.

The effect of average parameters on the emissions estimates of the median vessels in the sample was greater on load-factor-based models than on resistance-based models. This was especially true when considering the adoption of subtype averaged total install propulsive power values. Total installed propulsive power has a large amount of variance. Of the resistance-based models, the Kristensen method was most sensitive to the use of average displacement. Hull displacement is often under-represented and requires gap-filling in most ship registry databases.

Whereas the adoption of all subtype average ship parameters may result in a 20 percent difference in emissions estimates for typical vessels, the adoption of just one average parameter results in at most a 10 percent difference. This analysis concludes that the application of average values for a single parameter is typically more accurate than the application of those for all parameters.

Discussion

The availability of AIS data has allowed access to more accurate and detailed ship speed and reported draft information. In correlation with this, more complex, load-factor-based, and resistance-based, power models have recently been applied to marine emissions inventories. An understanding of the effect of these models, and the required gap-filling on their input parameters, is necessary for future inventory comparisons and analysis. This is significant, as future modeling efforts will reflect the growing impact of shipping on worldwide greenhouse gas emissions and the future global marine fuel sulfur cap (International Maritime Organization, 2014).

Fleet-wide emissions inventories were significantly impacted by power model selection and were minimally impacted by the use of subtype averaged ship parameters. Any transition away from the commonly used Propeller Law resulted in decreased emissions, likely because the Propeller Law is equivalent to assuming maximum hull wetted surface area. Similarly, most transitions from load-factor-based, to resistance-based, models resulted in decreased modeled emissions. This result agrees with the IMO Third Greenhouse Gas Study, which saw the load factor exponent (n) increase, and modeled power decrease, when equating load-factor-based and resistance-based model results (International Maritime Organization, 2014). A comparison of these power models across speed ranges displayed how load-factor-based models are rooted in their proportionality parameters, c and n. In assuming these to be constant, load-factor-based models may be representative near service speeds, when frictional resistance dominates total hull resistance. However, their failure to account for wave-making resistance is especially significant at high speeds, when wave-making resistance heavily impacts power demand. These results agree with industry publications on the effect of wave-making resistance estimated by resistance-based models (MAN Diesel & Turbo, 2011) (Schneekluth, 1998). Only high-speed or fully-loaded vessel activities, plotted in Figure 7, were modeled as requiring greater power by resistance-based

methods than by the Propeller Law. It is thus concluded that the results of similar analysis on a sample fleet with much faster activity profiles, or much heavier loads, would differ significantly from that of the current study.

Resistance-based models have often been avoided due their large number of required inputs. This analysis shows that subtype averaged ship parameters may be applied to ship specific activities to get relatively accurate emissions estimates (within 2.5 percent). Inventory sensitivities to average values increase as sample size decreases. It is worth noting that this study did not assess the spatial distribution of emissions. For air quality modeling purposes, the impact of averaging ship parameters may be different within a given modeled grid cell.

Container ships, tankers, and bulk carriers are comprised of generally well-defined ship groups and subtypes, with limited hull design options. Because of this, future analysis is required to understand the effect of subtype average ship parameters on more variable ship groups, such as Ro-Ros and passenger ships. Likewise, resistance-based models allow for a wide range of modeling opportunities which were not considered in this analysis. These include modeling for the impacts of acceleration, shallow water operations, variable sea water temperature, and ship trim, among others (Jalkanen, 2014) (Lackenby, 1963) (Schneekluth, 1998). Service, fouling, and weather margins were excluded from this analysis for simplicity sake, however their inclusion is recommended for any power model implementation in emissions modeling (Harvald, 1982) (International Maritime Organization, 2014) (Kristensen, 2016) (MAN Diesel & Turbo, 2011). Analysis of outlier vessels showed that fully-loaded and high-speed vessels would likely be modeled with larger emissions by resistance-based methods than load-factor based methods. The speed profiles in the baseline fleet (Figure 1) indicate that the analyzed inventories were largely impacted by slow-speed activity due to the Los Angeles and Long Beach vessel speed reduction zones. Because of this, future analysis should compare the effects of power models on regions without vessel speed reduction zones for a greater understanding of power model influences on emissions inventories.

Acknowledgements

The authors would like to thank Mr. Rex Roebuck of the U.S. Coast Guard Navigation Center for facilitating our access to the NAIS data set used in this study. They would also like to thank Mr. Hans Otto Kristensen for his support in accessing and understanding the SHIP-DESMO excel models.

This project was supported in part by an appointment to the Internship/Research Participation Program at the Office of Transportation and Air Quality, U.S. Environmental Protection Agency, administered by the Oak Ridge Institute for Science and Education through an interagency agreement between the U.S. Department of Energy and EPA. This paper may not necessarily reflect the views of the USEPA and no official endorsement should be inferred.

About the Authors

Isabela N. Brown is an ORISE research participant conducting research at the U.S. Environmental Protection Agency’s National Vehicle and Fuel Emissions Laboratory in Ann Arbor, MI.

Michael F. Aldridge is a physical scientist at the U.S. Environmental Protection Agency’s National Vehicle and Fuel Emissions Laboratory in Ann Arbor, MI.

Sources

Diesel & Gas Turbine Publications. “2013 Global Sourcing Guide.” 2013

EPA. “Regulatory Impact Analysis: Control of Emissions f Air Pollution from Category 3 Marine Diesel Engines,” 2009a.

EPA, ICF. “Current Methodologies in Preparing Mobile Source Port-Related Emission Inventories,” 2009b.

Goldsworthy Laurie, and Brett Goldsworthy. “Modelling of Ship Engine Exhaust Emissions in Ports and Extensive Coastal Waters Based on Terrestrial AIS Data – An Australian Case Study.” Environmental Modelling & Software 63 (1 2015): 45–60. 10.1016/j.envsoft.2014.09.009.

Harvald Sv.Aa. Resistance and Propulsion of Ships Wiley Interscience, 1983.

International Maritime Organization. “Third IMO GHG Study 2014 - Final Report.” London: International Maritime Organization, 2014.

IHS Maritime Fairplay. “IHS Fairplay Lloyds Data.” https://maritime.ihs.com/EntitlementPortal/Home/Index, accessed 2014.

Holtrop J, and Mennen GGJ. “An Approximate Power Prediction Method,” 1982.

Jalkanen J-P, Johansson L, Kukkonen J, Brink A, Kalli J, and Stipa T. “Extension of an Assessment Model of Ship Traffic Exhaust Emissions for Particulate Matter and Carbon Monoxide.” Atmospheric Chemistry and Physics 12, no. 5 (3 12, 2012): 2641–59. 10.5194/acp-12-2641-2012.

Jalkanen Jukka-Pekka, Johansson Lasse, and Kukkonen Jaakko. “A Comprehensive Inventory of the Ship Traffic Exhaust Emissions in the Baltic Sea from 2006 to 2009.” AMBIO 43, no. 3 (4 2014): 311–24. 10.1007/s13280-013-0389-3. [PubMed: 23479266]

Kristensen Hans Otto. “Resistance and Propulsion Power,” 2016.

Kristensen Hans Otto. “Revision of Statistical Analysis and Determination of Regression Formulas for Main Dimensions of Bulk Carriers Based on Data from Clarkson,” (2017a).

Kristensen Hans Otto. “Revision of Statistical Analysis and Determination of Regression Formulas for Main Dimensions of Container Ships Based on Data from Clarkson,” (2017b).

Kristensen Hans Otto. “Revision of Statistical Analysis and Determination of Regression Formulas for Main Dimensions of Tankers Based on Data from Clarkson,” (2017c).

Kristensen Hans Otto. “Ship-Desmo-Tool.” Accessed 7 6th, 2017d https://gitlab.gbar.dtu.dk/oceanwave3d/Ship-Desmo/tree/master

Lackenby H “The Effect of Shallow Water on Ship Speed.” The Shipbuilder and Marine-Engine Builder, 9 1963.

MacKay Jim, Sturtz Timothy M., Lindhjem Christian, Chan Lit, and Yarwood Greg. “Final Report Link-Based Modeling Emissions Inventory of Marine Vessels (Ocean Going Vessels) in Transit and at Anchor in the Gulf of Mexico.” Contract 582 (2015): 15–50417.

MAN Diesel & Turbo “Basic Pricipals of Propulsion,” 2011.

Molland Anthony F., Turnock Stephen R., and Hudson Dominic A.. Ship Resistance and Propulsion: Practical Estimation of Ship Propulsive Power New York: Cambridge University Press, 2011.

Nunes RAO, Alvim-Ferraz MCM, Martins FG, and Sousa SIV. “The Activity-Based Methodology to Assess Ship Emissions - A Review.” Environmental Pollution 231 (12 2017): 87–103. 10.1016/j.envpol.2017.07.099. [PubMed: 28793241]

Rakke Stian Glomvik. “Ship Emissions Calculation from AIS.” NTNU, 2016 https://brage.bibsys.no/xmlui/handle/11250/2410741.

Scarbrough Tim, Tsagatakis Ioannis, Smith Kevin, and Wakeling Daniel. “A Review of the NAEI Shipping Emissions Methodology.” Ricardo Energy & Environment, 12 12, 2017.

Schneekluth H, and Volker Bertram Ship Design for Efficiency and Economy 2nd ed. Oxford; Boston: Butterworth-Heinemann, 1998.

Starcrest Consulting Group, LLC. “2014 Multi-Facility Emissions Inventory of Cargo Handling Equipment, Heavy-Duty Diesel Vehicles, Railroad Locomotives, and Commercial Marine Vessels.” Starcrest Consulting Group,LLC, 2 2016.

Starcrest Consulting Group, LLC. “Port of Los Angeles Inventory of Air Emissions-2016,” 9 2017.

United States Army Corps of Engineers. “2016 Entrances and Clearances” http://www.navigationdatacenter.us/data/dataclen.htm. (accessed 12 2017)

Whall C, Cooper D, Archer K, Twigger L, Thurston N, Ockwell D, McIntyre A, and Ritchie. A “Quantification of Emissions from Ships Associated with Ship Movements between Ports in the European Community (Part 2).” Cheshire: Entec UK Limited, 2002.

Yau PS, Lee SC, Corbett James J., Chengfeng Wang, Cheng Y, and Ho. KF “Estimation of Exhaust Emission from Ocean-Going Vessels in Hong Kong.” Science of The Total Environment 431 (8 2012): 299–306. https://doi.or201g/10.1016/j.scitotenv.2012.03.092. [PubMed: 22698572]

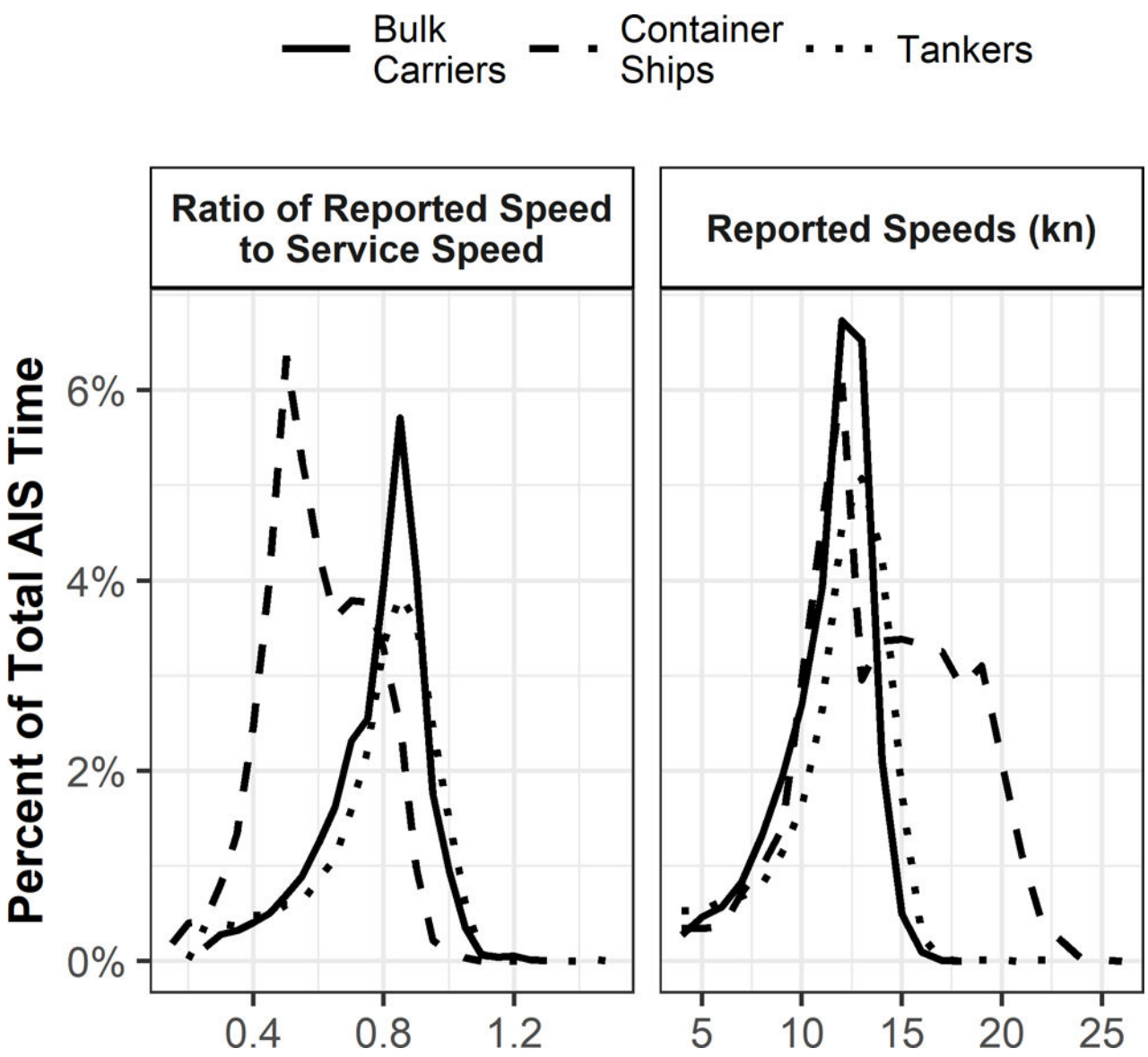

Figure 1.
Distribution of vessel speeds from AIS data, as a ratio of vessel service speed, and as reported.

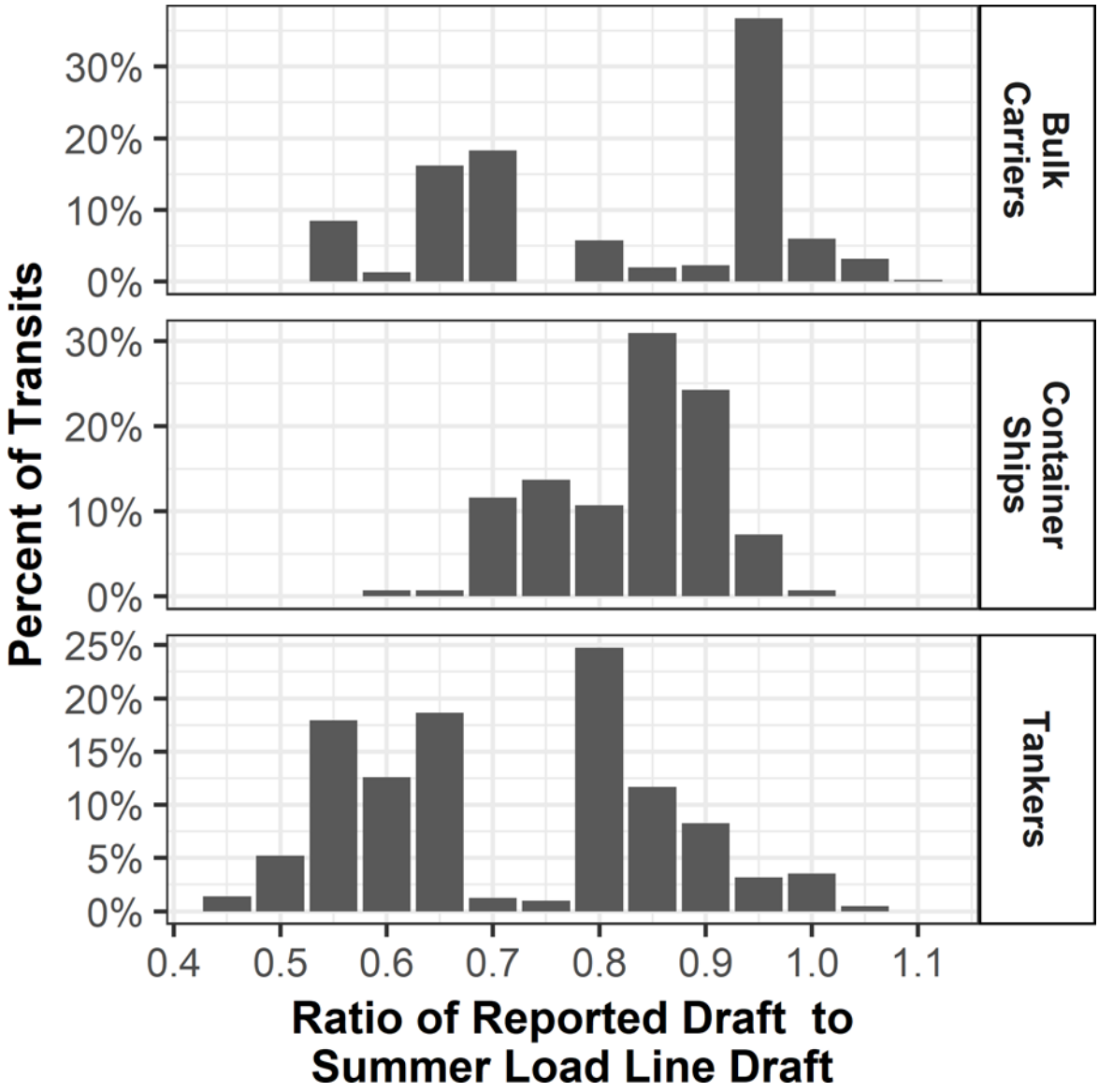

Figure 2.
Distribution reported vessel draft to summer load line draft for each ship type.

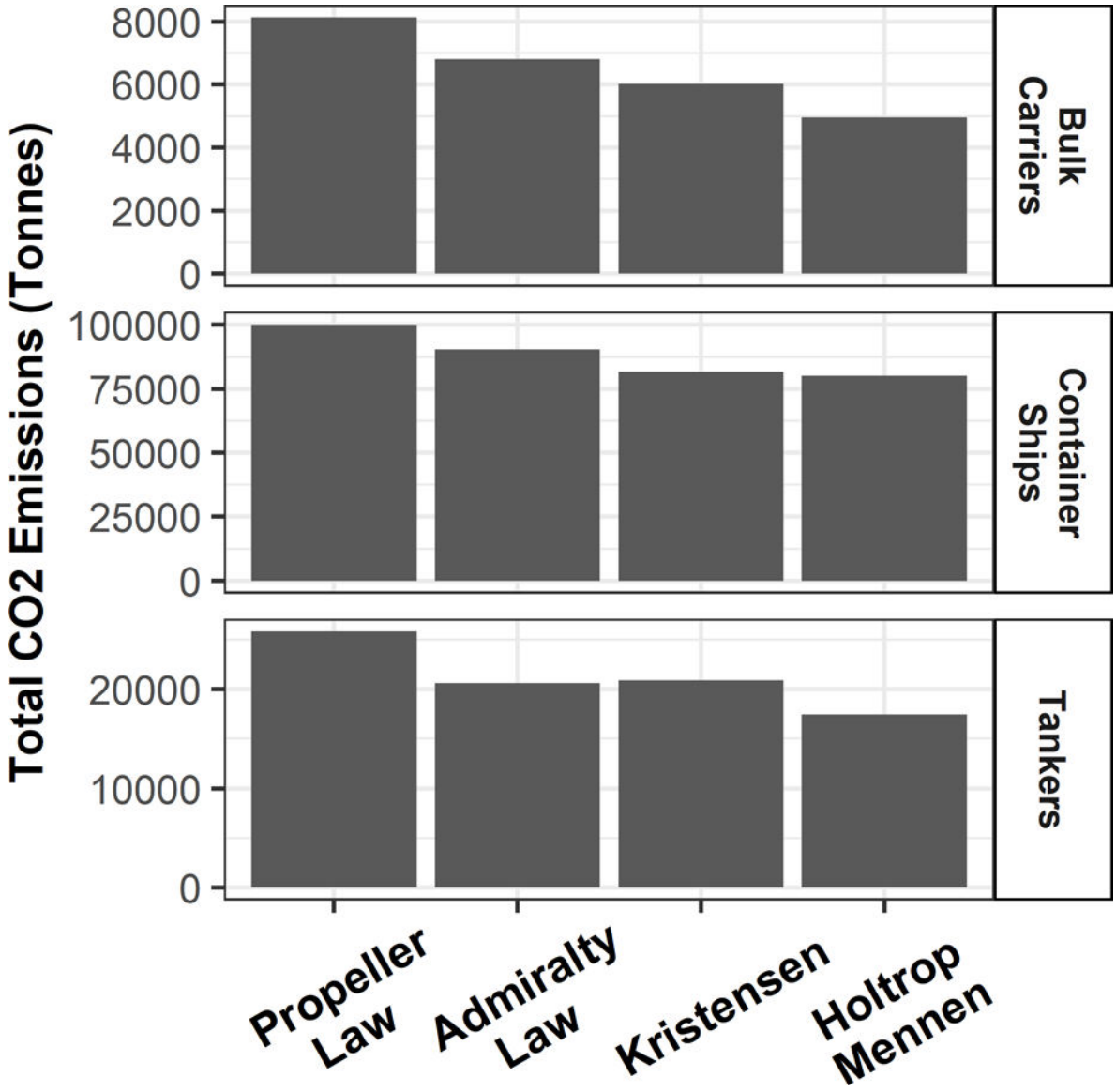

Figure 3.
Total CO_2 emissions calculated using each model, for each ship type.

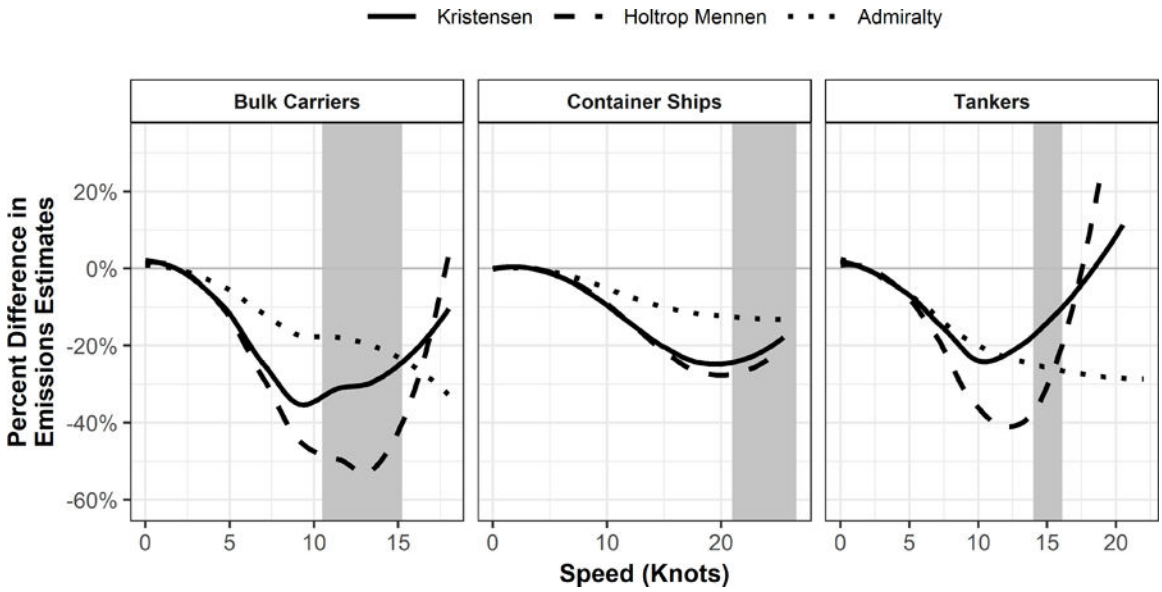

Figure 4.

Percent difference in emissions estimates for each model relative to the propeller law model. The shaded regions indicate the service speed range for each vessel type.

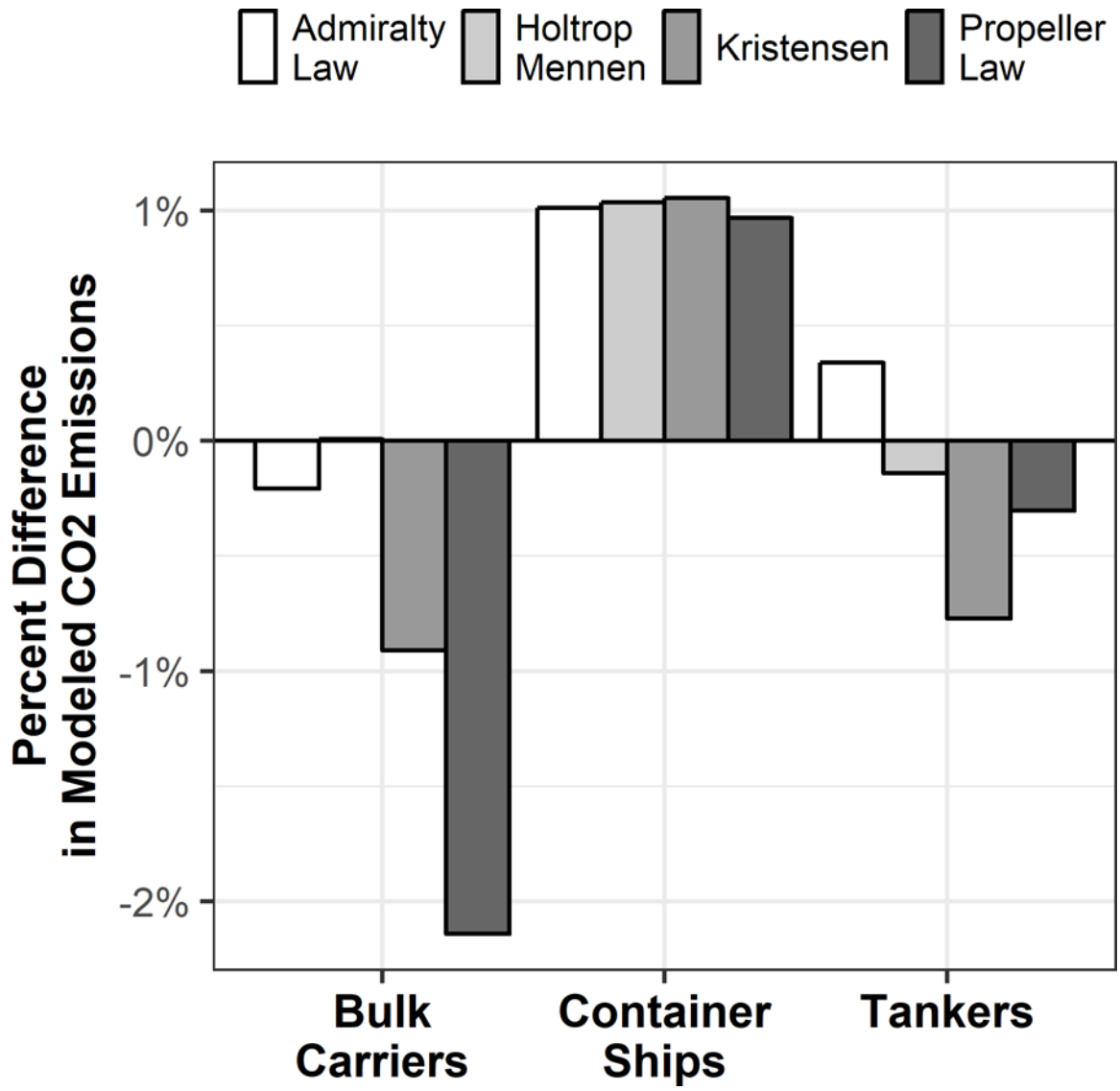

Figure 5.
Effect of using sub-type average hull parameters for estimating fleet level emissions

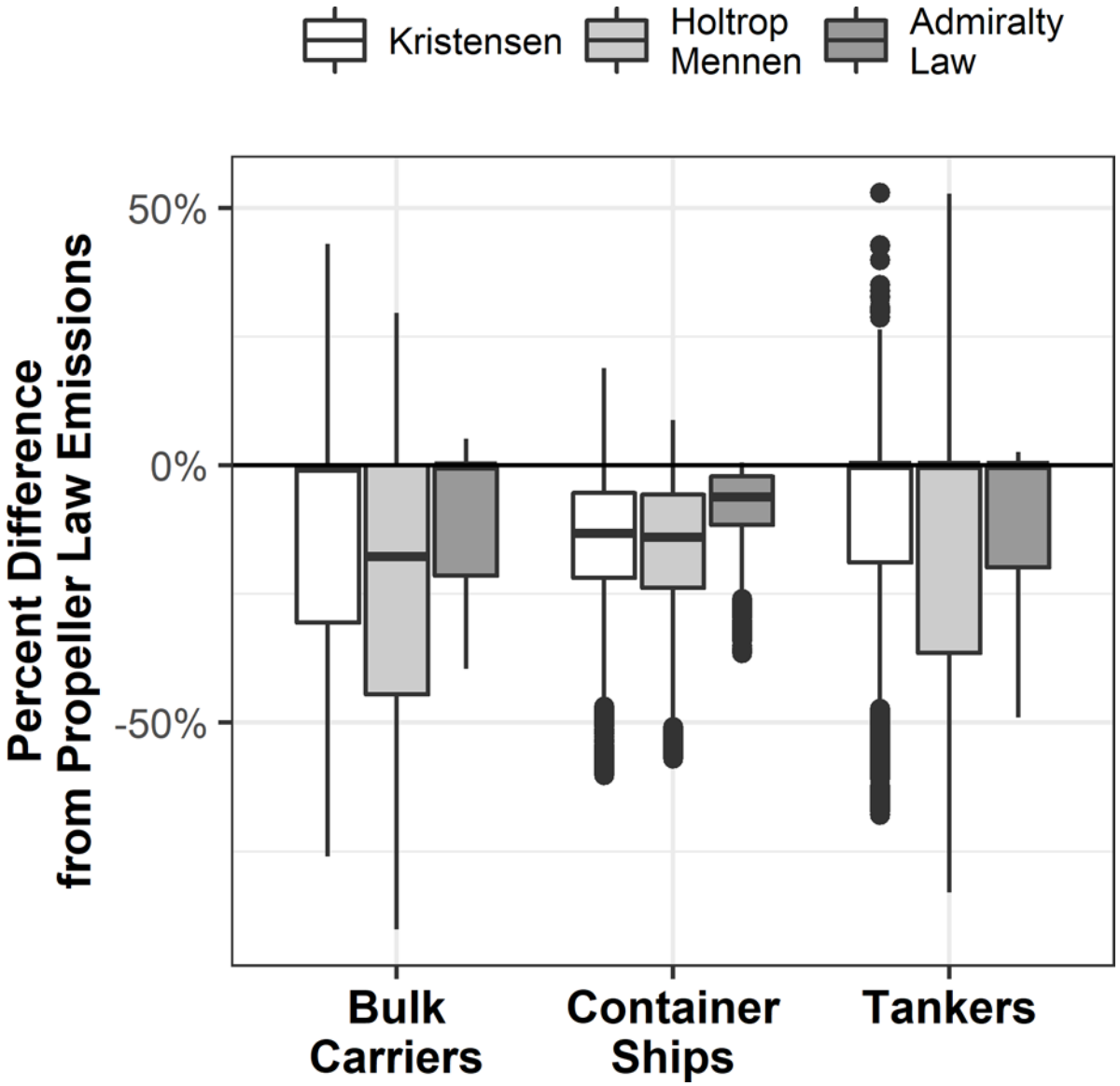

Figure 6.
Percent difference in estimated CO_2 emissions relative to the propeller law model for individual vessels

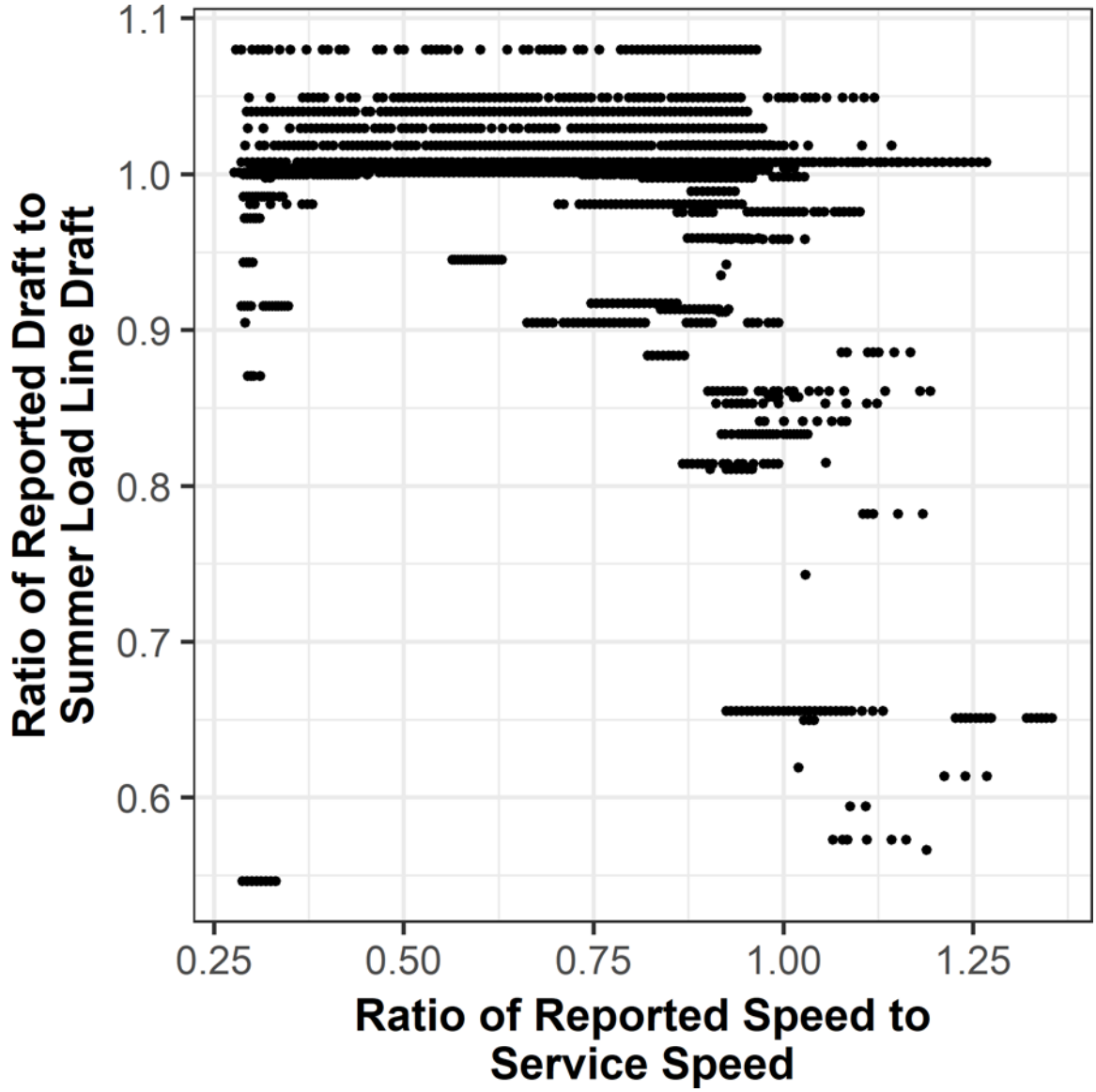

Figure 7.
Reported speed and draft conditions that resulted in propulsive power estimates greater than those generated by the propeller law

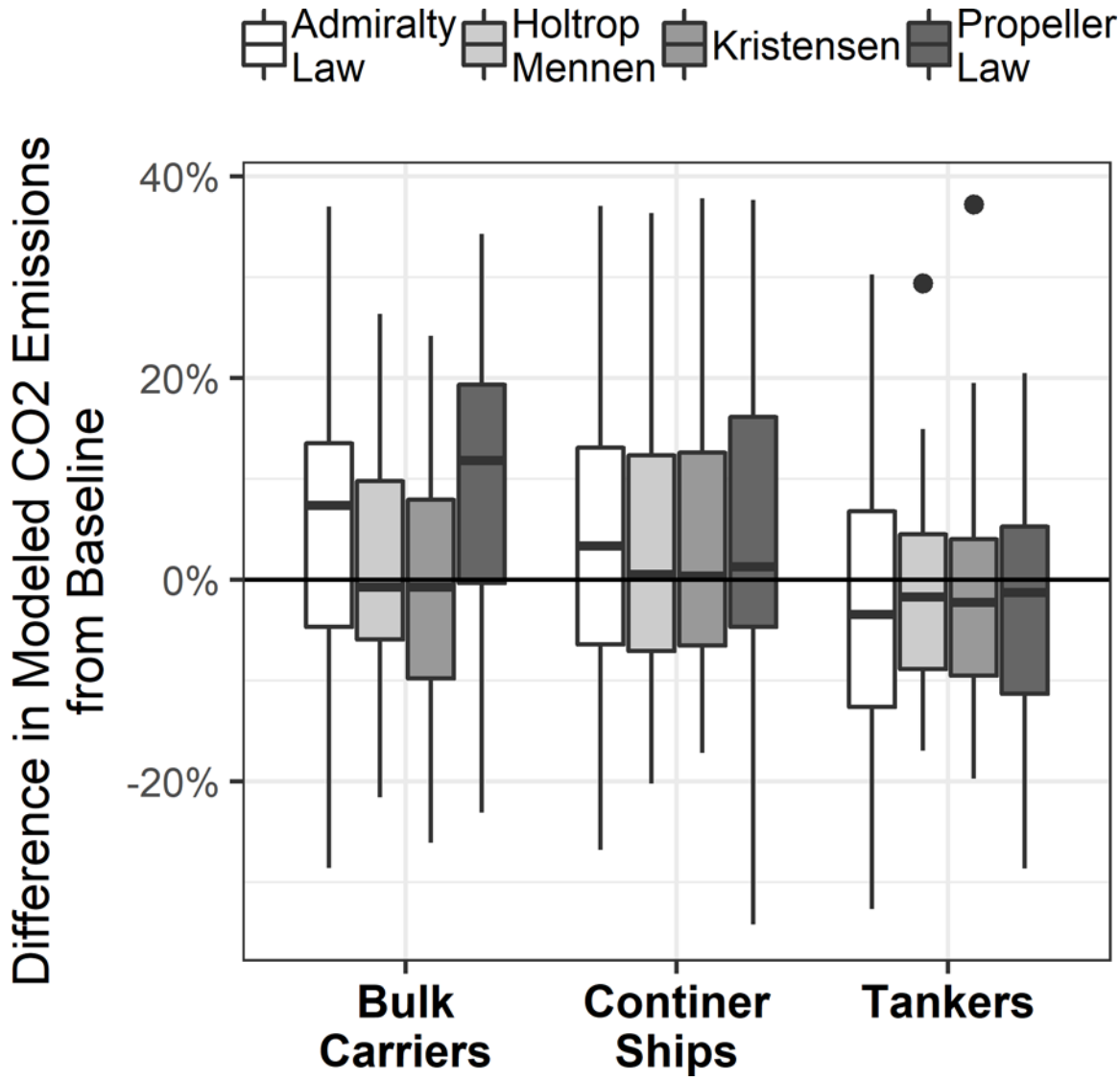

Figure 8.

Effect of using average hull parameters to calculate CO_2 emissions for a single ship, rather than using ship specific parameters.

Table 1:

Averaged ship parameters for bulk carriers

Subtype	**Handymax**	**Panamax**
Sample Size	24	21
DWT Range	25000– 55000	55000 – 85000
Reported Draft (m)	9.21 ± 17.19%	9.5 ± 16.37%
Breadth (m)	29.42 ± 3.6%	32.24 ± 0.1%
Displacement (m^3)	41971.8 ± 13.58%	80259.58 ± 10.31%
Service Speed (kn)	14.2 ± 3.67%	14.6 ± 1.69%
Summer Load Line Draft (m)	10.08 ± 6.92%	13.57 ± 4.24%
Total propulsive power (kW)	6614.04 ± 14.5%	11637.7 ± 21.12%
Block Coefficient	0.81 ± 1.72%	0.85 ± 1.1%
Waterline Length (m)	173.81 ± 2.84%	216.24 ± 7.23%
Deadweight Tonnage	34813.43 ± 15.4%	67777.13 ± 9.07%

Table 2:

Averaged ship parameters for container ships

Subtype	Feeder	Panamax	Post-Panamax
Sample Size	7	27	88
DWT Range	< 35000	35000 – 60000	> 60000
Reported Draft (m)	8.93 ± 9.4%	10.74 ± 9.11%	11.93 ± 10.54%
Breadth (m)	28.64 ± 5.94%	32.6 ± 5.23%	42.1 ± 10.22%
Displacement (m^3)	38679.11 ± 6.63%	62230.57 ± 12.66%	123881.07 ± 21.67%
Service Speed (kn)	21.38 ± 2.77%	22.96 ± 5.17%	24.73 ± 2.78%
Summer Load Line Draft (m)	11.36 ± 0.94%	12.39 ± 3.7%	14.4 ± 4.78%
Total propulsive power (kW)	20790.28 ± 9.57%	34308.41 ± 18.6%	60003.25 ± 16.84%
Block Coefficient	0.65 ± 7.45%	0.64 ± 3.63%	0.65 ± 4.33%
Waterline Length (m)	184.57 ± 6.54%	239.1 ± 8.14%	310.1 ± 8.24%
Deadweight Tonnage	29148.77 ± 7.15%	47604.12 ± 12.25%	94727.84 ± 22.11%

Table 3:

Averaged ship parameters for tankers

Subtype	Handysize	handymax	Panamax	Aframax	Suezmax	VLCC
Sample Size	6	26	35	9	1	4
DWT Range	10000 – 25000	25000 – 55000	55000 – 80000	80000 – 120000	120000 – 170000	> 170000
Reported Draft (m)	8.89 ± 11.94%	9.88 ± 18.47%	10.25 ± 17.83%	9.25 ± 2 1.44%	9.2 ± 0%	12.28 ± 28.48%
Breadth (m)	24.53 ± 2.56%	31.1 ± 6.73%	32.23 ± 0.09%	43.38 ± 1.83%	45.7 ± 0%	60 ± 0%
Displacement (m^3)	27072.37 ± 11.68%	51796.25 ± 19.5%	83384.08 ± 5.35%	128138.81 ± 3.86%	169844.88 ± 0%	358303.7 ± 0.38%
Service Speed (kn)	14.87 ± 1.03%	14.88 ± 2.85%	14.86 ± 3.34%	15.33 ± 1.72%	15.3 ± 0%	15.97 ± 1.51%
Summer Load Line Draft (m)	9.92 ± 5.84%	12.02 ± 8.98%	13.92 ± 4.64%	14.97 ± 0.37%	17.52 ± 0%	22.62 ± 0.21%
Total propulsive power (kW)	6636.51 ± 10.69%	8430.22 ± 14.22%	11420.38 ± 10.63%	13383.53 ± 3.55%	16858 ± 0%	29047.44 ± 3.17%
Block Coefficient	0.76 ± 0.59%	0.8 ± 2.44%	0.84 ± 0.78%	0.83 ± 1.28%	0.81 ± 0%	0.82 ± 0.11%
Waterline Length (m)	145.02 ± 3.54%	170.88 ± 5.4%	220.62 ± 1.45%	238.88 ± 2.24%	260.58 ± 0%	323.02 ± 0.12%
Deadweight Tonnage	20834.68 ± 6.95%	43331 ± 20.71%	71462.97 ± 5.01%	113092.03 ± 4.08%	151736 ± 0%	319350.77 ± 0.22%

Table 4:

Percent difference from Propeller Law estimated CO_2 emissions

Power Model	Bulk Carriers	Container Ships	Tankers
Admiralty Law	−15.62%	−9.5%	−18.1%
Kristensen	−26.19%	−19.17%	−17.06%
Holtrop Mennen	−42.37%	−20.67%	−30.53%